AWARD NUMBER: W81XWH-19-1-0265

TITLE: Overcoming Anti-PD-1 Resistance in Lung Cancer

PRINCIPAL INVESTIGATOR: Nejat Egilmez

CONTRACTING ORGANIZATION: University of Louisville

REPORT DATE: August 2020

TYPE OF REPORT: Annual

PREPARED FOR: U.S. Army Medical Research and Development Command
Fort Detrick, Maryland 21702-5012

REPORT DOCUMENTATION PAGE

Form Approved
OMB No. 0704-0188

1. REPORT DATE	2. REPORT TYPE	3. DATES COVERED
August 2020	Annual	8/1/2019 – 7/31/2020

4. TITLE AND SUBTITLE
Overcoming Anti-PD-1 Resistance in Lung Cancer

5a. CONTRACT NUMBER

5b. GRANT NUMBER
W81XWH-19-1-0265

5c. PROGRAM ELEMENT NUMBER

6. AUTHOR(S)
Nejat Egilmez

E-Mail:nejat.egilmez@louisville.edu

5d. PROJECT NUMBER

5e. TASK NUMBER

5f. WORK UNIT NUMBER

7. PERFORMING ORGANIZATION NAME(S) AND ADDRESS(ES)

Barbara Sells
University of Louisville
2301 S 3rd Street
Louisville, KY 40206

8. PERFORMING ORGANIZATION REPORT NUMBER

9. SPONSORING / MONITORING AGENCY NAME(S) AND ADDRESS(ES)

U.S. Army Medical Research and Development Command
Fort Detrick, Maryland 21702-5012

10. SPONSOR/MONITOR'S ACRONYM(S)

11. SPONSOR/MONITOR'S REPORT NUMBER(S)

12. DISTRIBUTION / AVAILABILITY STATEMENT

Approved for Public Release; Distribution Unlimited

13. SUPPLEMENTARY NOTES

14. ABSTRACT

The goal of this proposal was to first define the cellular and molecular effector mechanisms that underlie our original observation, i.e. lung Th17 immunity drives anti-PD-1 resistance in lung cancer(Aim1); and then determine whether the lung microbiota signature ultimately determines the severity of Th17 cell activity (Aim 2). To this end, we have constructed a genetic model that will allow us to test the central hypothesis, i.e. lung Th17 cells are the primary drivers of resistance to anti-PD-1 (Aim 1a). This model is now being assessed for functionality prior to directly testing the above notion. In addition, we found that the post-anti-PD-1 treatment Th17 cell prevalence in the cancerous lung is predictive of treatment outcome (Aim 1b). Finally, we have found that lung MDSC activity does not explain the anti-PD-1-Th17 cell driven treatment resistance (Aim 1ci) and are now exploring the other alternative mechanisms (Aim 1cii-iv). In the coming year we plan to conclude remaining Aim 1 work and initiate Aim 2 studies.

15. SUBJECT TERMS
Lung cancer, Anti-PD-1, IL-17, Th17 cells, microbiota

16. SECURITY CLASSIFICATION OF:			17. LIMITATION OF ABSTRACT	18. NUMBER OF PAGES	19a. NAME OF RESPONSIBLE PERSON
					USAMRMC
a. REPORT	b. ABSTRACT	c. THIS PAGE			19b. TELEPHONE NUMBER *(include area code)*
Unclassified	Unclassified	Unclassified	Unclassified		

TABLE OF CONTENTS

Page

INTRODUCTION

This is the first annual report for the above grant. The progress has been mostly consistent with the timelines of the SOW. Specifically, the studies outlined under Major Task 1, i.e. Subtasks 1, 2, 3 and 4 (partial), which were to be performed in year 1, have been completed with one exception. Subtask 2, which was to be performed during the months 3-9 is partially completed, due to the pandemic and the associated shutdowns. We plan to complete Subtasks 2/4 and initiate Major Task 2 studies in Year 2.

KEYWORDS

Lung cancer, anti-PD-1, IL-17, Th17 cells, microbiota.

ACCOMPLISHMENTS

***Specific Aim 1*. To define the cellular and molecular effector mechanisms that mediate anti-PD-1-Th17 cell axis-driven therapeutic resistance in the LSL-K-ras^{G12D} lung cancer model (Months 1-18)**.

Major Task 1: To confirm the effect of anti-PD-1 on lung-associated Th17 cells in the LSLKras spontaneous lung cancer model.

Subtask 1: Obtain ACURO approval. Establish the model and breed mice after approval has been issued (Months 1-3). This task was completed on schedule. CD4$^{Cre/ert2}$ and RORc$^{fl/fl}$ mice were purchased, expanded and then cross-bred to obtain CD4$^{Cre/ert2/+}$ RORc$^{fl/fl}$ mice in which administration of tamoxifen should result in the inactivation of RORc gene in CD4^{+} cells. Figure 1 shows a representative genotyping analysis of such mice.

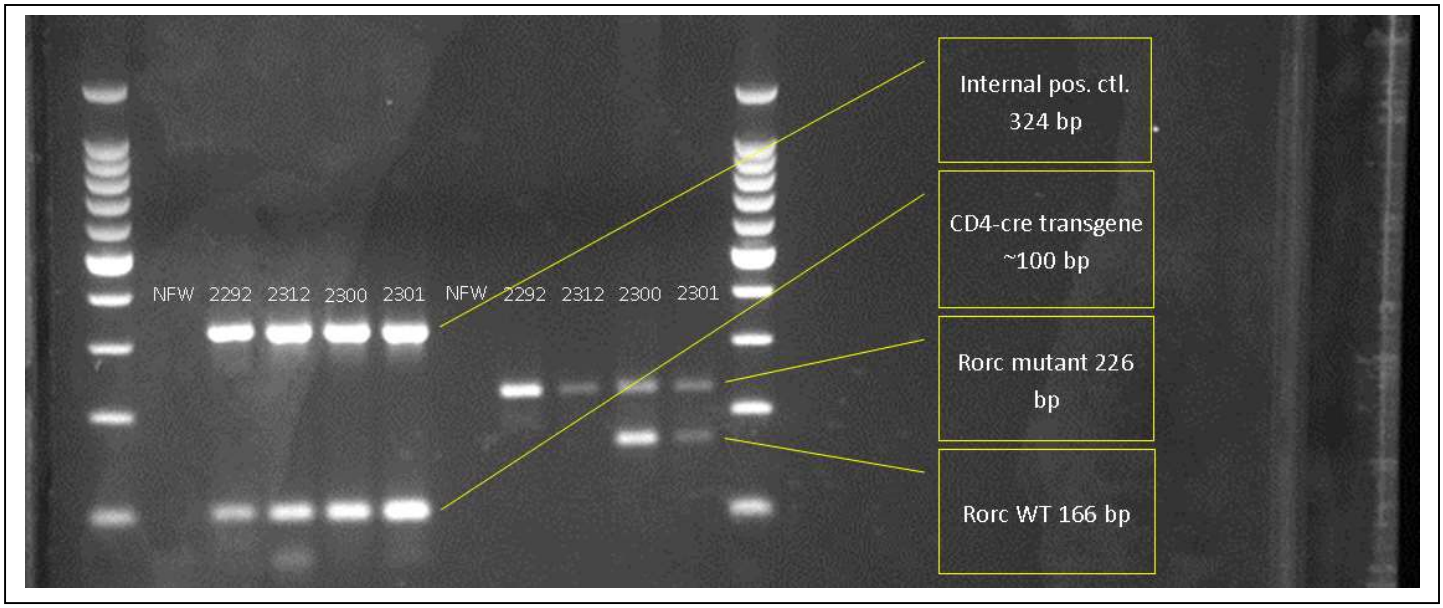

Figure 1. Genotyping of CD4^{Cre} x RORc$^{fl/fl}$ mice. Four representative mice with different genotyps are shown (2292, 2312, 2300 and 2301). Mice 2300 and 2301 represent the F1 generation (CD4$^{Cre/+}$ and RORc$^{fl/+}$) between the two homozygous mutant breeders (CD4$^{Cre/Cre}$ and RORc$^{fl/fl}$), containing one copy each of the transgenes. Mice 2292 and 2312 represent a successful backcross between an F1 mouse and the homozygous RORc$^{fl/fl}$ mouse yielding a CD4$^{Cre/+}$ heterozygous and a RORc$^{fl/fl}$ homozygous progeny.

Subtask 2: Is anti-PD-1-mediated enhancement of Th17 effector activity solely responsible for ICI resistance? (Months 3-9). The CD4$^{Cre/+}$RORc$^{fl/fl}$ mice described above are now being tested to determine whether tamoxifen administration will achieve effective excision of the RORc gene to eliminate RORc expression in CD4^{+} T-cells. Once this is confirmed, bone marrow from these mice will be engrafted into LSL-K-ras mice and tumors will be induced to study the effect of RORc elimination. This Aim has been delayed due to COVID19-related shutdown of the laboratories.

Subtask 3. Does Th17/CTL functional balance correlate with therapeutic efficacy? (Months 9-11). This task was completed. LSL-K-ras mice were analyzed individually for Th17, γδT17 and CD8^{+} T-cell prevalence and activity as well as tumor burden following anti-PD-1 + anti-IL-17 therapy. Regression analysis revealed a significant association between post-therapy lung Th17 cell prevalence and therapeutic outcome (Figure 2). In contrast, γδT17 and CTL prevalence, or the functional ratio of CTL to T17 subsets did not correlate with tumor burden (data not shown). These results establish that the post-treatment lung Th17 cell prevalence was the superior predictor of outcome in this model. These data have been incorporated into a manuscript, which was submitted to the Cancer Immunology Research as a Priority Brief in June of 2020 (Appendix).

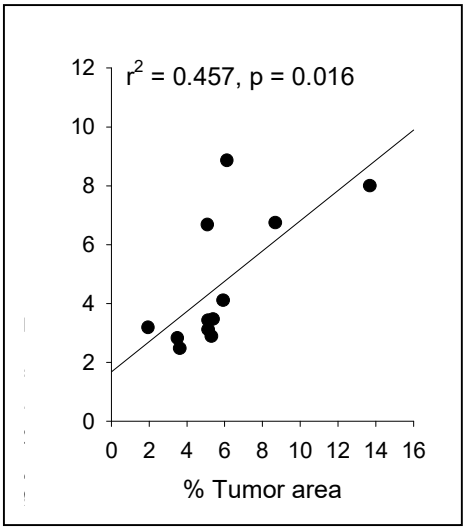

Figure 2. Correlation of Th17 cell prevalence and tumor burden in post-therapy mice. Individual mice were analyzed for tumor burden and Th17 cell prevalence after anti-PD-1 + anti-IL-17 treatment (n = 12). Regression analysis was performed (SigmaPlot 12) to determine significance.

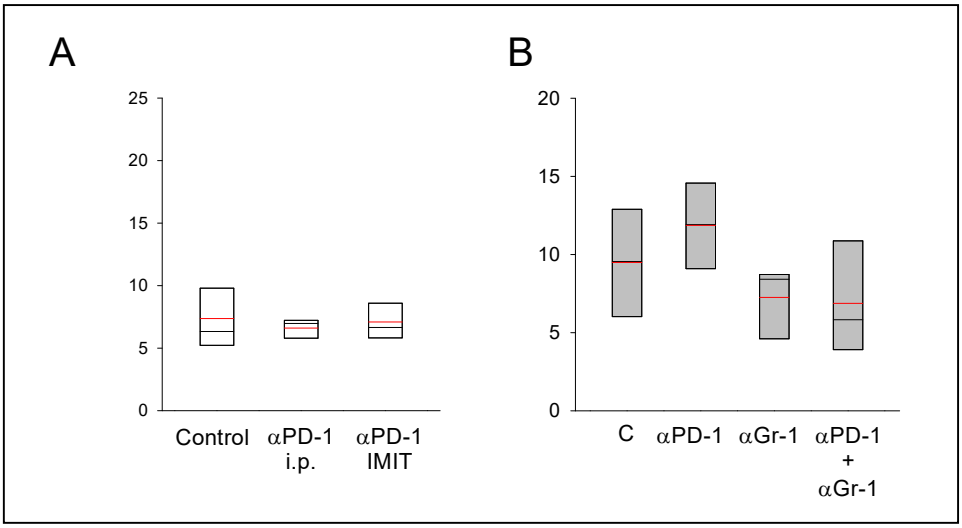

Figure 3. Role of MDSC in anti-PD-1 resistance. *Panel A*. Mice were analyzed for tumor burden and MDSC prevalence after anti-PD-1 antibody treatment. Anti-PD-1 was administered either as soluble antibody (100ug, ip in 0.1ml saline, 2x/wk, for 4 weeks starting at 6 weeks post-adeno^{Cre}; or via intratracheal (IMIT) administration of anti-PD-1-encapsulated polylactic acid microparticles (1 ug antibody, 2x/wk). There were no significant differences between the groups (n = 4-6/group). *Panel B*. Mice were administered anti-PD-1 (ip) and/or anti-Gr-1 antibody (100ug, ip). The differences between groups were not significant (n = 5/gp). Red line = mean, black line = median.

Subtask 4: How does anti-PD-1-Th17 axis counteract anti-PD-1-CTL axis? (Months 11-18). These studies were initiated recently and part (a) was completed.

a. Analyze myeloid cell subset prevalence in control vs anti-PD-1-treated mice. These studies were performed as planned. The prevalence of MDSC were analyzed in the tumor-bearing lungs (6 weeks post-adenovirus^{Cre}) of LSL-K-ras mice. Briefly mice were treated with anti-PD-1 antibody, either using soluble antibody or a slow-release formulation [encapsulated into biodegradable polylactic acid microspheres - administered via intubation-mediated intratracheal route (IMIT)]. The data shown in Figure 3A reveal that independent of the administration route, there was no effect on the MDSC. Similarly, treatment in the presence or the absence of MDSC (depletion via anti-Gr-1 antibody administration) did not overcome resistance. These data establish that MDSC do not play a significant role in anti-PD-1 resistance.
b. Repeat experimental group above in the presence or absence of IL-17 neutralization. Not started.
c. Analyze the effect of MDSC depletion on anti-PD1 treatment. Not started.
d. IL-17-mediated induction of PD-L1 expression. Not started.
e. IL-17-mediated tumor-cell proliferation. Not started.
f. IL-17-mediated pro-tumorigenic cytokine expression. Not started.

Specific Aim 2. **To delineate the role of lung microbiota in the ontogeny of tumor-elicited Th17 immunity and resistance to ICI therapy** (months 15-24). Not started.

Future work. In year 2 we plan to complete Aim 1 Subtask 2 as well as Subtask 4b-f experiments plus initiate the studies outlined in Aim 2. We anticipate that a no-cost extension (Year 3) will be needed to complete Aim 2 work due to the delays caused by the COVID19 outbreak.

IMPACT

The findings outlined above provide important tools and information in support of our central hypothesis. First, the availability of the new genetic construct will enable direct testing of the notion that lung-associated Th17 cells are central to anti-PD-1 resistance in the LSL-K-ras mouse model of lung cancer, thus providing unequivocal evidence for (or against) this idea. Second, the finding that post-anti-PD-1 therapy Th17 cell prevalence in the lungs is predictive of therapeutic outcome not only provides further support for our central hypothesis, but also establishes proof-of-principle for the potential use of Th17 cell density as a biomarker for responsiveness to treatment. Finally, the demonstration that MDSC do not play a role in Th17-driven resistance is novel and suggests that the underlying mechanism is more complex than anticipated. Collectively, these data will provide the premise, at least in part, of a future R01 type research grant application to the NIH.

CHANGES/PROBLEMS

In year 1, no changes were introduced to the original proposal. The only problem that was encountered was the COVID19 pandemic and the associated closure of University laboratories, which set us back by 4 months. We plan to ask for a one-year no-cost extension to ameliorate this issue.

PRODUCTS

N/A

PARTICIPANTS & OTHER COLLABORATING ORGANIZATIONS

There were no changes to the original proposal. No external collaborators were involved.

SPECIAL REPORTING REQUIREMENTS

N/A

APPENDICES

See attached draft manuscript.

Anti-PD-1 Antibody-mediated Activation of Type 17 T-Cells Undermines Checkpoint Blockade Therapy

Qingsheng Li[1, 3] *, Phuong T. Ngo[2, 3] and Nejat K. Egilmez[1, 3] *

Departments of [1]Microbiology & Immunology, and [2]Medicine, School of Medicine; [3]James Graham Brown Cancer Center, University of Louisville, Louisville, KY 40202.

Running title: Mechanisms of anti-PD-1 resistance in NSCLC

Keywords: anti-PD-1, NSCLC, IL-17, checkpoint blockade resistance, CD4 T-cell

This work was supported by the Department of Defense Lung Cancer Research Program Concept award W81XWH1610185 (NKE) and Idea award W81XWH1910265 (NKE).

*All correspondence should be addressed to: Nejat Egilmez or Qingsheng Li, Department of Microbiology and Immunology, School of Medicine, University of Louisville, 505 S.Hancock St., Louisville, Kentucky 40202, USA. Phone: (502) 852-5351, FAX: (502) 852-7531. Email: nejat.egilmez@louisville.edu or qingsheng.li@louisville.edu.

N.K.E has ownership interest in Therapyx, Inc. The remaining authors declare no competing financial interests.

Abstract

Tumors that develop in the genetic LSL-K-ras^{G12D} murine lung cancer model are resistant to anti-PD-1 antibody treatment. Analysis of tumor-bearing lungs from anti-PD-1-treated mice revealed an up to 2.5-fold increase in IL-17-producing T-cells, with minimal change in $CD8^+$ T-cell activity. Neutralization of IL-17 concurrent with anti-PD-1 treatment on the other hand, resulted in robust $CD8^+$ cytotoxic T-cell (CTL) activation and a 3-fold reduction in tumor burden. Loss-of-function studies demonstrated that both $CD4^+$ and $\gamma\delta TCR^+$ T-cells contributed to IL-17-mediated de-sensitization of CTL to anti-PD-1, and that CTL activation was critical to tumor eradication. Importantly, post-therapy lung Th17 cell prevalence prognosticated treatment efficacy. Consistent with the murine data, analysis of tumor biopsy samples from non-small cell lung cancer (NSCLC) patients revealed that intratumoral $CD8^+$ / $RORc^+$ cell ratio correlated with response to immune checkpoint blockade (ICB). These findings provide the initial evidence for a new mechanism of ICB resistance in lung cancer.

Introduction

Immune checkpoint inhibitors, in particular anti-PD-1 antibodies, represent a new paradigm in the management of NSCLC (1). At the same time, while effective in a subset of patients as first or second line therapy, anti-PD-1 still fails in 50-75% of NSCLC patients (1). High tumor PD-L1 expression and neoantigen burden correlate with anti-PD-1 responsiveness, and in part may explain the suboptimal response rates (1, 2). However, 30 to 40% of PD-L1-positive and high neoantigen burden tumors still do not respond while up to 14% of low neoantigen tumors do respond (3) suggesting that other, yet unidentified, factors contribute to resistance. To this end, the broader tumor immune signature, the functional ontogeny of tumor-infiltrating $CD8^+$ T-cells as well as the commensal microbiota have been identified as other contributors to responsiveness, but are yet to provide specific measurable prognostic markers in the clinical setting (2).

To gain further insight into this conundrum we investigated the therapeutic potential of anti-PD-1 antibody in the checkpoint blockade-resistant, low-neoantigen burden LSL-K-ras^{G12D} murine spontaneous lung cancer model (4-6). Anti-PD-1 antibody had no detectable therapeutic benefit in LSL-K-ras^{G12D} mice, confirming previous findings (6). Phenotypic and functional analyses of lung T-cell populations revealed that anti-PD-1 mediated activation of lung-intrinsic Type 17 T-cells (T17 cells) directly interfered with the ability of the antibody to activate antitumor CTL, and that post-therapy lung Th17 cell prevalence was predictive of therapeutic outcome in individual mice. Consistent with these findings, preliminary analysis of NSCLC patient tumor biopsies revealed a correlation between intratumoral $CD8^+$ / $RORc^+$ cell ratio and tumor responsiveness to ICB. This is the first report of a potential role for anti-PD1-mediated T17 activation in resistance to ICB.

Materials and Methods

Mice and tumor model. LSL-K-ras^{G12D} (B6.129S4-Krastm4Tyj/J) mice were purchased from The Jackson Laboratory (Bar Harbor, ME). Tumors were induced as described previously (7). All experiments were approved by the University IACUC.

Patient samples. De-identified NSCLC patient tumor biopsy specimens were obtained from the Brown Cancer Center Biorepository, University of Louisville. Tissue sections prepared from formalin-fixed, paraffin-embedded tumor samples were processed for RNAscope. The study was approved by the University Institutional Review Board.

Microsphere preparation and treatment. Anti-PD-1 antibody-encapsulated biodegradable polylactic acid microspheres were prepared as previously described (7). Two formulations were produced: 1) control (no antibody) and 2) anti-mouse CD279 (PD-1) antibody (clone J43, BioXCell, West Lebanon, NH) with a loading of 8 μg antibody/mg of particles. Control or anti-PD-1 microspheres (0.1 mg particles in 35 μl sterile water) were administered via intubation-mediated intratracheal instillation (IMIT) 2x/week for 4 weeks starting 6 weeks after adenoviral infection (7). Soluble antibody (200 μg in 0.2ml saline) was administered i.p. 3x/week.

In vivo antibody-mediated leukocyte subset depletion and cytokine neutralization. Depletion was performed by i.p. injection of 250 μg of anti-mouse CD4 (clone GK1.5), CD8 (clone 53-6.72, BioXCell) or via i.v. injection of γδTCR antibody (clone UC7-13D5, BioXCell or Leinco Technologies) 3x/week for 4 weeks. For in vivo neutralization of IL-17, 100 μg anti-mouse IL-17A (clone 17F3; BioXCell) was administered i.p. 3x/week for 4 weeks.

Tumor quantification. Lung tumor burden was quantified by digital imaging analysis of H&E-stained serial lung sections as described previously (7). QuPath open source software was used to quantify lesion vs total lung area per section.

Isolation of lung mononuclear cells. Lung mononuclear cells were isolated as previously described (7).

Antibodies and flow cytometry. Fluorescence-conjugated anti-CD4 (RM4-5), anti-CD8a (53-6.7), anti-γδTCR (GL3), anti-CD11b (M1/70), anti-Gr-1 (RB6-8C5), anti-Ly-6G (1A8), anti–IL-17A (TC11-18H10.1), anti–IFN-γ (XMG1.2) and anti-RORγt (Q31-378), were purchased from BioLegend (San Diego, CA), eBioscience (Waltham, MA) or BD Biosciences (San Jose, CA). Foxp3 (PJK-16s; eBioscience) was quantified by intracellular staining performed according to the manufacturer's protocol. For intracellular cytokines, cells were stimulated for 4h with PMA and ionomycin (Sigma-Aldrich, St. Louis, MO) in the presence of brefeldin A (Sigma-Aldrich) and stained with antibodies. For CD107a degranulation assay, cells were cultured in RPMI1640 with anti-CD3 (10 µg/ml) and anti-CD28 (1 µg/ml) in 96-well plates for 24 h; were washed and re-stimulated with PMA and ionomycin in the presence of anti-CD107a (1D4B, BioLegend) for an additional 4 h.

Single-molecule RNA in situ hybridization. RNAscope (8) was performed at Advanced Cell Diagnostics (Newark, CA). Briefly, manual chromogenic staining was performed with paired double-Z oligonucleotide probes for CD8a green (cat. no. 560391) and RORc red (cat. no. 556991) using RNAscope® 2.5 HD Duplex Reagent Kit (cat. no. 322430) per manufacturer's instructions. Each sample was quality controlled for RNA integrity with a probe specific to peptidylpropyl isomerase B. Negative control background staining was evaluated using a probe specific to the bacterial dapB gene. Stained slides were scanned with Aperio ScanScope slide scanner at 40x objective resolution (Aperio Technologies, Vista, CA). High-resolution images taken with ObjectiveView (Digital Pathology Image Viewer) and TIFF images were then subjected to computerized analysis with Fuji software to quantify positive cells per field.

Statistical analysis. Student's t-test was used to determine the significance of the differences between control and experimental groups in pairwise comparisons. In experiments with multiple groups, homogeneity of intergroup variance was analyzed by one-way ANOVA with multiple pairwise comparisons using Tukey or Holm-Sidak analyses. A p value of <0.05 was considered significant.

Results

Failure of anti-PD-1 therapy is associated with exacerbation of T17 activity

We previously demonstrated that intratracheal (i.t.) delivery of a sustained-release IL-10 formulation, but not systemic bolus cytokine, suppressed lung tumorigenesis in the LSL-K-ras^{G12D} model (7). To this end, we wanted to determine whether a similar formulation of anti-PD-1 antibody could overcome ICB-resistance in these mice. Animals with established lung adenomas were administered either the slow-release formulation or soluble anti-PD-1 i.t. or intraperitoneally (i.p.), respectively. Analysis of lung tumor burden in post-therapy mice demonstrated that treatment failed with either approach (Figure 1A). To gain further insight into the observed lack of effect, global analysis of lung immune cell infiltrates was undertaken. Immune phenotyping of lung lymphocytes in treated vs control mice revealed a variable effect on CD8$^+$ T-cell cytotoxicity, which did not reach statistical significance (Figure 1B). In contrast, we observed significant 2- and 1.3-fold increases in Th17 and γδT17 cell activity, respectively, in mice treated with i.t., but not i.p., antibody (Figure 1B). A minor but significant reduction in Th1 cells was also observed in mice receiving encapsulated antibody while no changes were detected in the prevalence of Treg or the myeloid cell subsets (Supplementary Figure 1).

Neutralization of IL-17 sensitizes LSL-K-ras^{G12D} lung tumors to anti-PD-1 therapy

Next, we wanted to determine whether exacerbation of T17 immunity interfered with the ability of anti-PD-1 to stimulate CD8$^+$ T-cell activity. Anti-PD-1 treatment in the presence of IL-17 neutralization resulted in effective tumor suppression in mice that received i.t., but not i.p. anti-PD-1 antibody (Figure 2A). To gain further insight into the synergy, we examined the post-therapy lung T-cell landscape. Phenotypic analysis of single cell preparations revealed that, in contrast to anti-PD-1 monotherapy which had no effect on CD8$^+$ T-cells, anti-IL-17 + i.t. anti-PD-1 (but not i.p. anti-PD-1) treatment increased CD8$^+$ T-cell cytotoxicity in the lung by 2-fold (Figure 2A); suggestive of an antagonistic relationship between type 17 immunity and CTL reinvigoration.

Since neutralization of IL-17 alone can result in reduced tumor growth in the LSLKras^{G12D} lung cancer model (9), we next determined whether combinatorial treatment was superior to anti-IL-17 alone (using i.t. anti-PD-1 from this point on). Figure 2B data show that while IL-17 blockade alone resulted in a trend towards reduced tumor burden, statistical significance was reached only in the combination group with a >3-fold reduction in tumor burden in comparison to controls. Consistent with this finding, analysis of lung T-cell subsets revealed that combination therapy resulted in more effective CTL activation than anti-IL-17 alone.

Th17 and γδT17 subsets contribute to anti-PD-1 resistance via distinct pathways

Next, we investigated the relative roles of Th17 and γδT17 cells in anti-PD-1 resistance. Tumor-bearing mice were treated with anti-PD-1 in the presence or absence of CD4$^+$ or γδTCR$^+$ T-cells and tumor burden was analyzed. Administration of anti-PD-1 antibody to CD4$^+$ T-cell-depleted mice resulted in significant tumor suppression in comparison to CD4-sufficient mice (Figure 3A), while depletion of CD4$^+$ T-cells alone had no effect. We thus concluded that anti-PD-1-mediated activation of CD4$^+$ T-cells played an important role in conferring resistance to therapy. In the case of γδTCR$^+$ cell subset however, depletion alone was just as effective as depletion + anti-PD-1 treatment in comparison to anti-PD-1 alone, suggesting that constitutive IL-17 production by γδT-cells contributed to anti-PD-1 resistance (Figure 3A).

In parallel, analysis of CD8$^+$ T-cells for membrane CD107a in mice that received anti-PD-1 in the absence or presence of CD4+ T-cells revealed that only the former group displayed significant CTL cytotoxicity (Figure 3A) while CD4$^+$ T-cell depletion alone had no benefit. These data suggested that anti-PD-1-mediated CD4$^+$ T-cell activation interfered with CTL reinvigoration and tumor kill, consistent with the tumor burden data. In the complementary study, analysis of post-therapy CTL cytotoxicity in γδT-cell deficient vs sufficient mice indicated that anti-PD-1 induced significant CTL activation in the absence of γδTCR$^+$ cells (Figure 3A). However, unlike what was observed with CD4$^+$ T-cells, depletion of γδT-cells in the absence of anti-PD-1 also resulted in partial CTL activation, again consistent with a role for constitutive IL-17 production by these cells in anti-PD-1 resistance.

Based on these findings, treatment was undertaken in mice with dual depletion of $CD4^+$ and $\gamma\delta TCR^+$ cells to determine whether this approach would replicate the IL-17-neutralization data. Treatment resulted in a ~2.5-fold reduction in tumor burden with a concurrent 2-fold increase in CTL cytotoxicity in $CD4^+$ and $\gamma\delta TCR^+$ T-cell depleted mice (Figure 3A) consistent with the IL-17-blockade data. Combined depletion in the absence of treatment was also partially effective suggesting that constitutive IL-17 production, likely by γδT17 cells, maintained CTL suppression at steady-state.

CTL are critical to the ability of anti-PD-1 to induce tumor eradication in the presence of IL-17 neutralization

As the data supported a strong link between CTL activation and tumor suppression, we next performed a loss of function study to directly test this notion. Mice with established disease were treated with anti-IL-17 + anti-PD-1 antibodies in the presence or absence of $CD8^+$ T-cells. Elimination of $CD8^+$ T-cells led to a complete loss of therapeutic efficacy confirming that tumor eradication was strictly dependent on CTL (Figure 3B).

Post-therapy Th17 cell prevalence is prognostic of treatment outcome in LSLKras^{G12D} mice

Above findings suggested that T17 cell prevalence/activity could prognosticate treatment outcome. To this end, mice were analyzed individually for Th17, γδT17 and $CD8^+$ T-cell prevalence and activity as well as tumor burden following combinatorial therapy. Regression analysis revealed a significant association between post-therapy Th17 cell prevalence and therapeutic outcome (Figure 3C). In contrast, γδT17 and CTL prevalence, or the functional ratio of CTL to T17 subsets did not correlate with tumor burden (Supplementary Figure 2A).

Tumor $CD8^+$/ $RORc^+$ cell ratio correlates with checkpoint blockade responsiveness in NSCLC patients

To determine whether we could extend the murine findings to human, pre-treatment lung tumor biopsy samples of NSCLC patients who subsequently received ICB therapy (Supplementary Table 1), were analyzed

198 for $CD8^+$ and $RORc^+$ cell infiltrates by RNAscope (Figure 4). Quantitative analysis revealed a statistically
199 significant correlation between the ratio of $CD8^+$ to $RORc^+$ cells and response to therapy. On the other hand,
200 in contrast to the murine model, $RORc^+$ cell prevalence alone was not predictive of ICB responsiveness
201 (Supplementary Figure 2B).

Discussion

Our data establish that the failure of anti-PD-1 therapy in the LSL-K-ras^{G12D} model is associated with an unexpected exacerbation of lung T17 cell activity that in turn antagonizes CD8$^+$ T-cell reinvigoration. We further demonstrate that Th17 cells are the major responders to anti-PD-1 and that post-treatment Th17 cell prevalence is predictive of therapeutic efficacy in individual mice. Importantly, preliminary analysis of NSCLC patient lung samples revealed a statistically significant correlation between tumor CD8$^+$/RORc$^+$ cell ratio and subsequent ICB responsiveness, consistent with the murine data. We propose that the intensity of the anti-PD-1-Th17 cell axis may be an important determinant of ICB resistance.

The finding that both CD4$^+$ and γδTCR$^+$ T-cells contribute to IL-17-mediated CTL unresponsiveness, but that Th17 cells are the primary prognosticators of outcome for anti-PD-1 treatment is an intriguing observation. Our data suggest that constitutive production of IL-17 by γδT-cells vs anti-PD-1-dependent activation of quiescent Th17 cells may underlie this observation. One caveat is that some of our conclusions regarding the Th17 subset were derived from studies involving total CD4$^+$ T-cell depletion, which cannot exclude potential contribution from T-regulatory cells. However, based on: a) the identification of IL-17 as the central mediator of anti-PD-1 resistance, and b) the nearly identical effects of IL-17 blockade and combined CD4$^+$ + γδTCR$^+$ cell depletion on anti-PD-1 efficacy, we expect T-regulatory cells to play a minor role in ICB resistance in this model.

ICB resistance of LSL-K-ras^{G12D} lung tumors (6, 10, 11) has been attributed to low neoantigen burden (5) and suboptimal CTL activity (12). At the same time, others have reported the presence of significant CD8$^+$ T-cell infiltrates in the tumor-bearing lungs of LSL-K-ras^{G12D} mice (13). Our findings suggest that these tumors are intrinsically immunogenic and that the CD8$^+$ T-cell infiltrates represent a bona fide antitumor response. Whether the observed CTL response in this model is driven by the G12D mutation (14-16) or involves other epitopes is yet to be determined.

IL-17 is a pleiotropic cytokine that can promote tumor growth directly or indirectly (17). However, the mechanistic basis of the IL-17-CTL antagonism remains to be elucidated. Potential mechanisms include the IL-17-MDSC axis (18, 19), direct proliferative effects of IL-17 on dysplastic epithelial cells (20), and/or increased PD-L1 expression on epithelium (21).

An intriguing observation that arose from this study was that anti-PD-1 antibody was effective only when delivered locally as a sustained release formulation. A similar observation was previously made with IL-10 (7) suggesting that in this ICB resistant model, i.p. injection may not achieve the therapeutic threshold in the lung, even in the presence of IL-17 blockade. Whether inhalable slow-release formulations represent a more effective alternative to i.v. antibody in individuals that are intrinsically resistant to ICB treatment is to be determined.

The prognostic data obtained in the murine model and the patient samples were conceptually consistent in that type 17 immunity was predictive of response in both. At the same time distinct markers, i.e. post-therapy Th17 cell prevalence in the case of mice and pre-therapy tumor $CD8^+$ / $RORc^+$ cell ratio in patients, associated with responsiveness. Several factors including post- vs. pre-therapy analysis or total lung vs intratumoral assessment of cell populations (in mice vs humans, respectively); patient neoantigen and PD-L1 heterogeneity; and/or the limited patient cohort could all account for the differences observed. Regardless, our findings support a novel role for anti-PD-1-T17 axis in mediating resistance to ICB in lung cancer.

References

1. Proto C, Ferrara R, Signorelli D, Lo Russo G, Galli G, Imbimbo M*, et al.* Choosing wisely first line immunotherapy in non-small cell lung cancer (NSCLC): what to add and what to leave out. Cancer Treat Rev **2019**;75:39-51 doi 10.1016/j.ctrv.2019.03.004.

2. Tunger A, Sommer U, Wehner R, Kubasch AS, Grimm MO, Bachmann MP*, et al.* The Evolving Landscape of Biomarkers for Anti-PD-1 or Anti-PD-L1 Therapy. J Clin Med **2019**;8(10) doi 10.3390/jcm8101534.

3. Rizvi NA, Hellmann MD, Snyder A, Kvistborg P, Makarov V, Havel JJ*, et al.* Cancer immunology. Mutational landscape determines sensitivity to PD-1 blockade in non-small cell lung cancer. Science **2015**;348(6230):124-8 doi 10.1126/science.aaa1348.

4. Jackson EL, Willis N, Mercer K, Bronson RT, Crowley D, Montoya R*, et al.* Analysis of lung tumor initiation and progression using conditional expression of oncogenic K-ras. Genes Dev **2001**;15(24):3243-8 doi 10.1101/gad.943001.

5. McFadden DG, Politi K, Bhutkar A, Chen FK, Song X, Pirun M*, et al.* Mutational landscape of EGFR-, MYC-, and Kras-driven genetically engineered mouse models of lung adenocarcinoma. Proc Natl Acad Sci U S A **2016**;113(42):E6409-E17 doi 10.1073/pnas.1613601113.

6. Pfirschke C, Engblom C, Rickelt S, Cortez-Retamozo V, Garris C, Pucci F*, et al.* Immunogenic Chemotherapy Sensitizes Tumors to Checkpoint Blockade Therapy. Immunity **2016**;44(2):343-54 doi 10.1016/j.immuni.2015.11.024.

7. Li Q, Anderson CD, Egilmez NK. Inhaled IL-10 Suppresses Lung Tumorigenesis via Abrogation of Inflammatory Macrophage-Th17 Cell Axis. J Immunol **2018**;201(9):2842-50 doi 10.4049/jimmunol.1800141.

8. Wang F, Flanagan J, Su N, Wang LC, Bui S, Nielson A et. al. RNAscope: A Novel in Situ RNA Analysis Platform for Formalin-Fixed, Paraffin-Embedded Tissues. J. Molec. Diagn. **2012** Jan;14(1):22-9. doi: 10.1016/j.jmoldx.2011.08.002.

9. Chang SH, Mirabolfathinejad SG, Katta H, Cumpian AM, Gong L, Caetano MS*, et al.* T helper 17 cells play a critical pathogenic role in lung cancer. Proc Natl Acad Sci U S A **2014**;111(15):5664-9 doi 10.1073/pnas.1319051111.

10. Ritzmann F, Jungnickel C, Vella G, Kamyschnikow A, Herr C, Li D, *et al*. IL-17C-mediated innate inflammation decreases the response to PD-1 blockade in a model of Kras-driven lung cancer. Sci Rep. 2019 Jul 17;9(1):10353. doi: 10.1038/s41598-019-46759-8.

11. Koyama S, Akbay EA, Li YY, Herter-Sprie GS, Buczkowski KA, Richards WG*, et al.* Adaptive resistance to therapeutic PD-1 blockade is associated with upregulation of alternative immune checkpoints. Nat Commun **2016**;7:10501 doi 10.1038/ncomms10501.

12. DuPage M, Cheung AF, Mazumdar C, Winslow MM, Bronson R, Schmidt LM*, et al.* Endogenous T cell responses to antigens expressed in lung adenocarcinomas delay malignant tumor progression. Cancer Cell **2011**;19(1):72-85 doi 10.1016/j.ccr.2010.11.011.

13. Busch SE, Hanke ML, Kargl J, Metz HE, MacPherson D, Houghton AM. Lung Cancer Subtypes Generate Unique Immune Responses. J Immunol **2016**;197(11):4493-503 doi 10.4049/jimmunol.1600576.

14. Tran E, Ahmadzadeh M, Lu YC, Gros A, Turcotte S, Robbins PF*, et al.* Immunogenicity of somatic mutations in human gastrointestinal cancers. Science **2015**;350(6266):1387-90 doi 10.1126/science.aad1253.

15. Cafri G, Yossef R, Pasetto A, Deniger DC, Lu YC, Parkhurst M*, et al.* Memory T cells targeting oncogenic mutations detected in peripheral blood of epithelial cancer patients. Nat Commun **2019**;10(1):449 doi 10.1038/s41467-019-08304-z.

16. Tran E, Robbins PF, Lu YC, Prickett TD, Gartner JJ, Jia L*, et al.* T-Cell Transfer Therapy Targeting Mutant KRAS in Cancer. N Engl J Med **2016**;375(23):2255-62 doi 10.1056/NEJMoa1609279.

17. Kuen DS, Kim BS, Chung Y. IL-17-Producing Cells in Tumor Immunity: Friends or Foes? Immune Netw **2020**;20(1):e6 doi 10.4110/in.2020.20.e6.

18. He D, Li H, Yusuf N, Elmets CA, Li J, Mountz JD*, et al.* IL-17 promotes tumor development through the induction of tumor promoting microenvironments at tumor sites and myeloid-derived suppressor cells. J Immunol **2010**;184(5):2281-8 doi 10.4049/jimmunol.0902574.

19. Akbay EA, Koyama S, Liu Y, Dries R, Bufe LE, Silkes M*, et al.* Interleukin-17A Promotes Lung Tumor Progression through Neutrophil Attraction to Tumor Sites and Mediating Resistance to PD-1 Blockade. J Thorac Oncol **2017**;12(8):1268-79 doi 10.1016/j.jtho.2017.04.017

20. Wang K, Kim MK, Di Caro G, Wong J, Shalapour S, Wan J*, et al.* Interleukin-17 receptor a signaling in transformed enterocytes promotes early colorectal tumorigenesis. Immunity **2014**;41(6):1052-63 doi 10.1016/j.immuni.2014.11.009.

21. Ma YF, Chen C, Li D, Liu M, Lv ZW, Ji Y*, et al.* Targeting of interleukin (IL)-17A inhibits PDL1 expression in tumor cells and induces anticancer immunity in an estrogen receptor-negative murine model of breast cancer. Oncotarget **2017**;8(5):7614-24 doi 10.18632/oncotarget.13819.

Figure Legends

Figure 1. Effect of anti-PD-1 treatment on tumor growth and lung T-lymphocyte activity. ***A***. *Tumor burden*. Tumor-bearing mice were treated with soluble or encapsulated anti-PD-1 and lungs were analyzed for tumor burden. Representative lung histology (left upper) with accompanying QuPath analysis identifying tumor areas (left lower, in red) and quantitative data (right) are shown (IMIT: intubation-mediated intratracheal instillation). There were no significant differences between the groups (n = 8-10 per group). ***B***. *T-cell activity*. Single cell suspensions prepared from the lungs were analyzed for cytotoxic $CD8^+$ T-lymphocytes ($CD8^+CD107a^+$), Th17 cells ($CD4^+ROR\gamma t^+IL\text{-}17^+$) and γδT17 cells ($\gamma\delta TCR^+ROR\gamma t^+IL\text{-}17^+$). Representative flow cytometry panels and quantitative data are shown (n = 5 per group). Boxes have lines at the median (black) and mean (red) showing lower (25%) and upper (75%) quartiles. Whiskers extend to show the 10^{th} and 90^{th} percentiles with symbols representing the extreme values (in groups with $n \geq 9$). Significance: ** denotes $p < 0.01$ (one-way ANOVA with pairwise multiple comparisons, Holm-Sidak).

Figure 2. Effect of IL-17 neutralization on anti-PD-1 therapy. ***A.*** *Effect of dual antibody treatment on tumor suppression and CTL cytotoxicity*. Tumor-bearing mice were treated with anti-PD-1 alone i.p (soluble antibody) or via IMIT (slow-release formulation) in the presence or absence of IL-17 neutralization. Tumor burden (n = 8-14 per group) and quantitative cellular data (n = 4-5 per group) including representative flow cytometry panels are shown. ***B.*** *Effect of IL-17 neutralization alone vs dual treatment*. Mice were treated with control blank microspheres, anti-IL-17 alone (i.p.), anti-PD-1 alone (encapsulated, via IMIT) or with anti-IL-17 + anti-PD-1. Tumor burden and cellular analysis data are shown (n = 5 per group). Significance: *, ** and *** denote $p \leq 0.05$, 0.01 and 0.001, respectively (one-way ANOVA with pairwise multiple comparisons, Dunn's or Holm-Sidak).

Figure 3. Roles of T17 and CTL in tumor responsiveness and prognosis. ***A.*** *Roles of $CD4^+$ and $\gamma\delta TCR^+$ cells*. Tumor burden was evaluated in mice that were treated with anti-PD-1 in the presence or absence of single or dual subset depletion; or subset depletion alone. Control mice received blank microspheres without

T-cell depletion. Top and bottom panels display the effect of depletion on tumor burden and CTL activity, respectively (n = 4-6 per group). ***B.*** *Role of CTL*. Mice were treated (Rx) with anti-PD-1 (IMIT) + anti-IL-17 (i.p.) in the presence or absence of CD8+ T-cell depletion. Control mice received blank microspheres (n = 8-13 mice per group). ***C.*** *Correlation of Th17 cell prevalence and tumor burden in post-therapy mice*. Individual mice were analyzed for tumor burden and Th17 cell prevalence after anti-PD-1 + anti-IL-17 treatment (n = 12). Box plots: *, ** and *** denote $p \leq 0.05$, 0.01 and 0.001, respectively (one-way ANOVA with pairwise multiple comparisons, Holm-Sidak).

Figure 4. Analysis of patient tumor $CD8^+$ and $RORc^+$ cell infiltrates. Tissue sections prepared from tumor biopsies were analyzed for CD8a (blue-green) and RORc (red) mRNA by RNAscope. A representative image is shown on the left (magnification = 400X). Cells expressing CD8a or RORc are highlighted with circles of relevant color. Inset displays magnification of the area demarcated by the rectangle. The average ratio of $CD8^+$ to $RORc^+$ cell numbers were calculated for each patient sample and plotted according to response criteria (right panel). The difference between Responders (progression free survival > 180 days, n = 3) and Non-responders (n = 6) was significant ($p < 0.01$, Student's t-test).

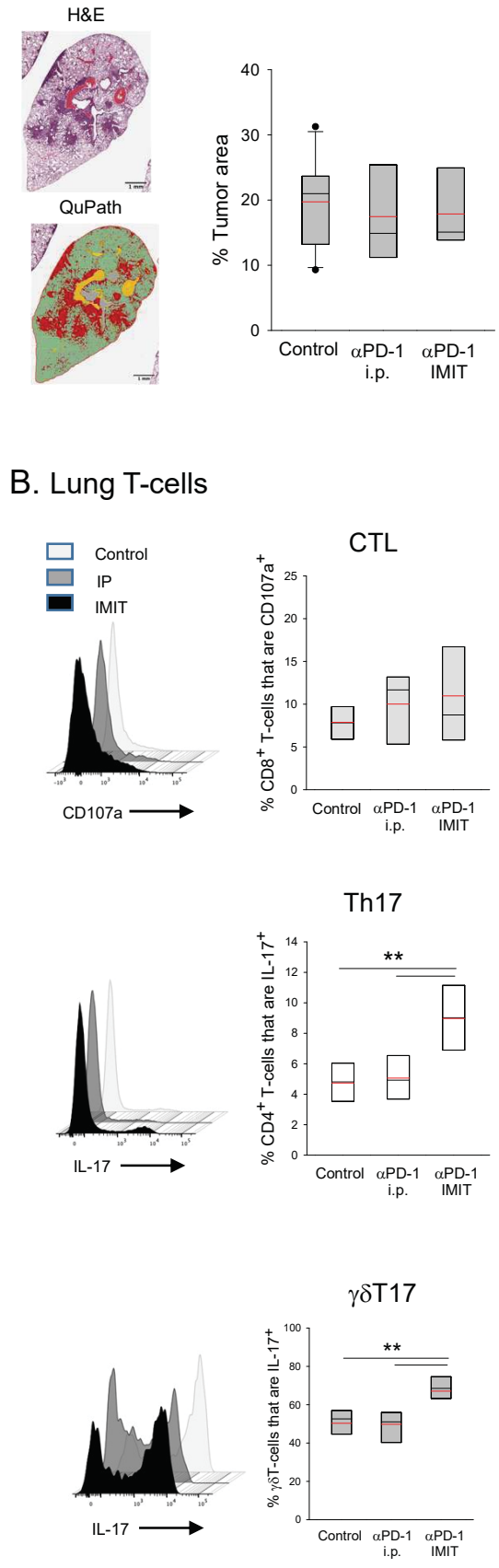
A. Tumor growth
H&E
QuPath
% Tumor area
40
30
20
10
0
Control
αPD-1 i.p.
αPD-1 IMIT
B. Lung T-cells
Control
IP
IMIT
CD107a
CTL
% CD8+ T-cells that are CD107a+
25
20
15
10
5
0
Control
αPD-1 i.p.
αPD-1 IMIT
IL-17
Th17
% CD4+ T-cells that are IL-17+
**
14
12
10
8
6
4
2
0
Control
αPD-1 i.p.
αPD-1 IMIT
IL-17
γδT17
% γδT-cells that are IL-17+
**
100
80
60
40
20
0
Control
αPD-1 i.p.
αPD-1 IMIT

Figure 1

A. Sensitization of tumor to anti-PD-1 by anti-IL-17

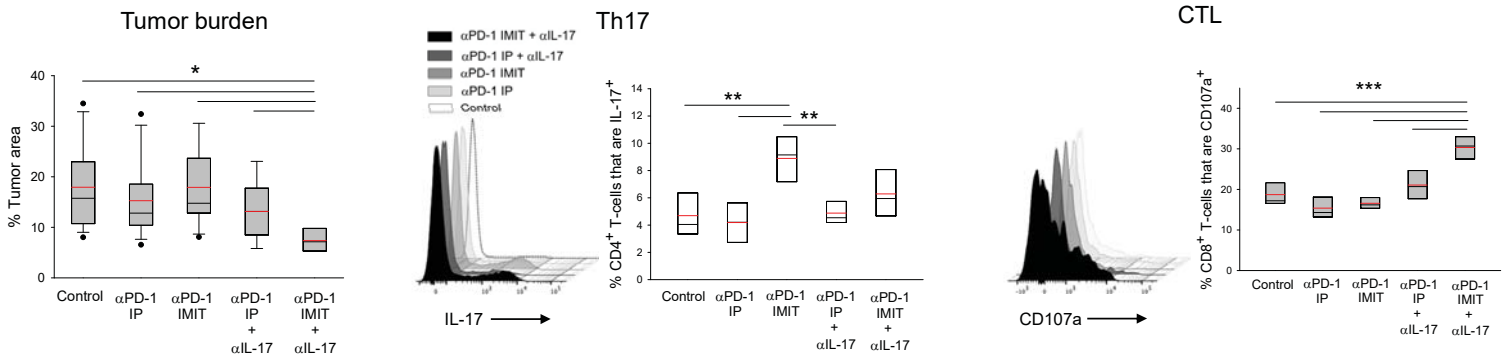

B. Efficacy of anti-IL-17 alone vs anti-IL-17 + anti-PD-1

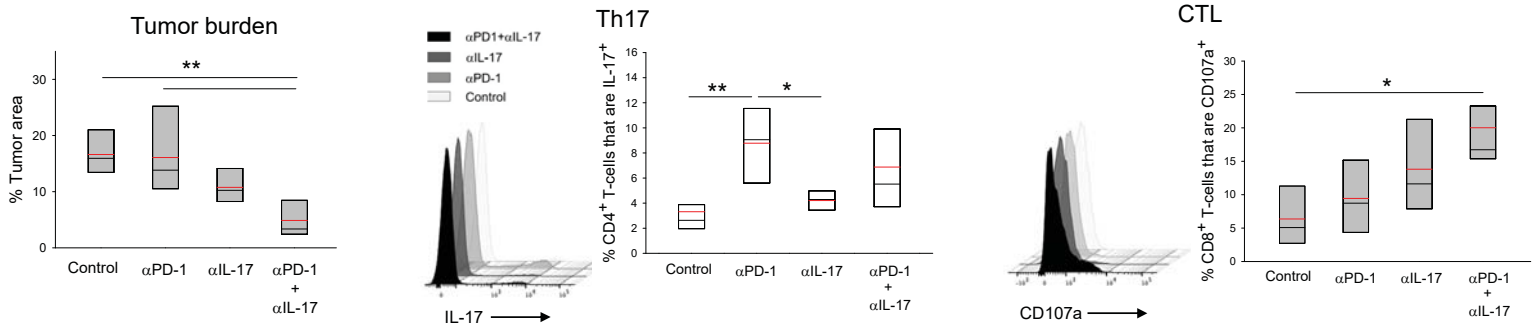

Figure 2

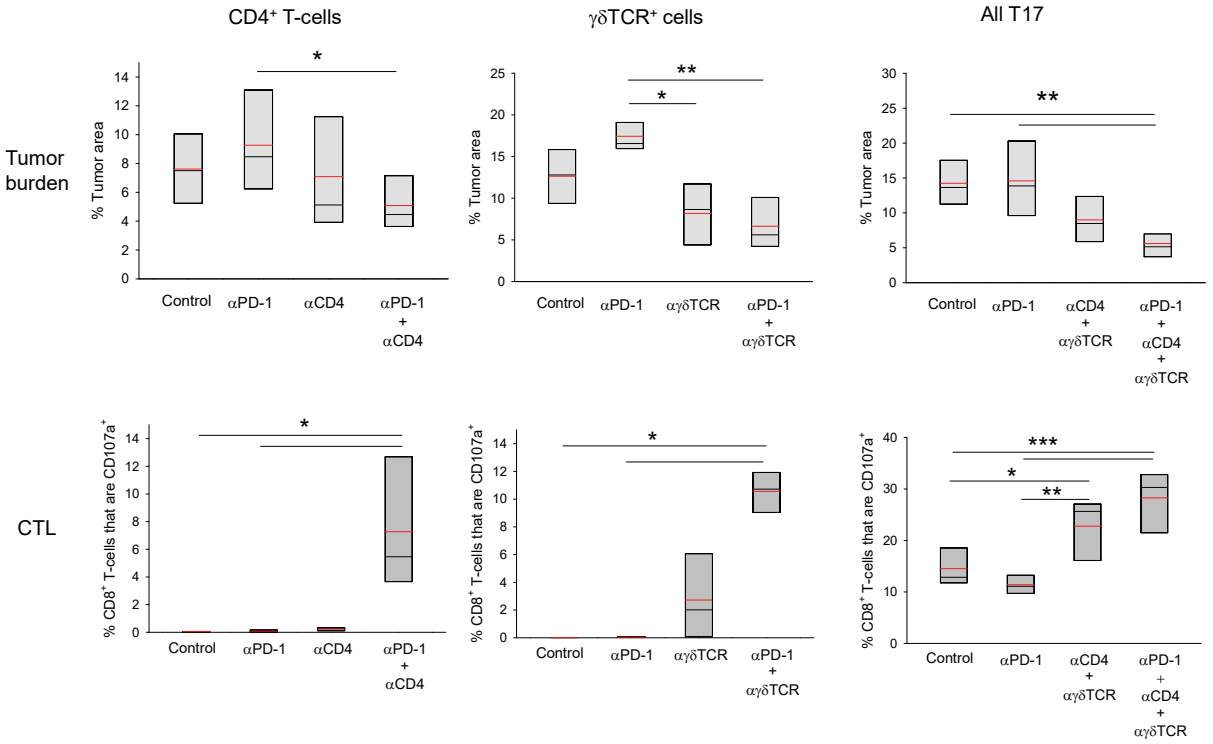
A. Role of T17 cells
CD4⁺ T-cells
γδTCR⁺ cells
All T17
Tumor burden
CTL
% Tumor area
% CD8⁺ T-cells that are CD107a⁺
Control
αPD-1
αCD4
αγδTCR
αPD-1 + αCD4
αPD-1 + αγδTCR
αCD4 + αγδTCR
αPD-1 + αCD4 + αγδTCR

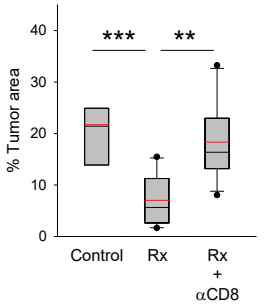
B. Role of CTL
% Tumor area
Control
Rx
Rx + αCD8

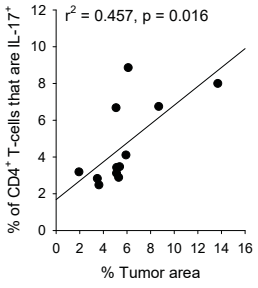
C. Tumor prognosis
r² = 0.457, p = 0.016
% of CD4⁺ T-cells that are IL-17⁺
% Tumor area

Figure 3

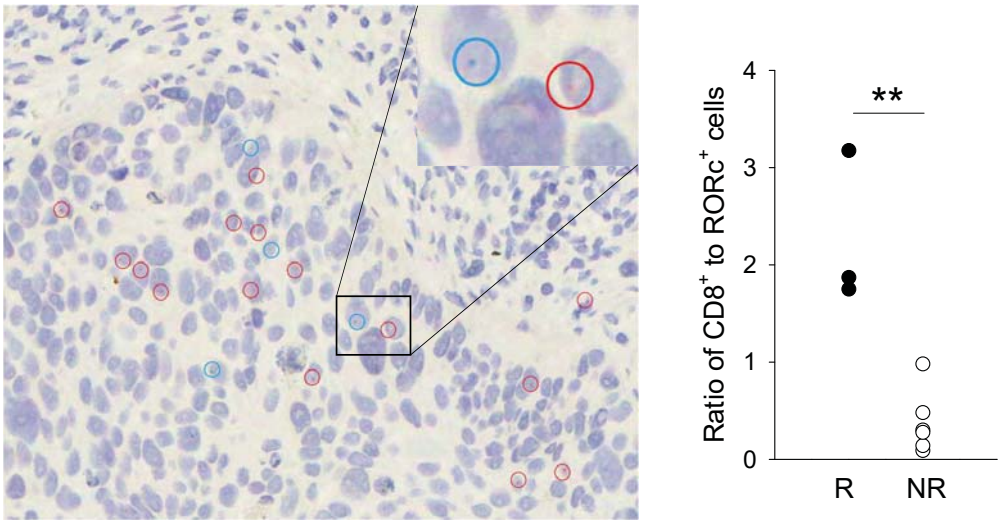

Figure 4